Article

Discovery Medicine 2025; 37(202): 2786–2802
https://doi.org/10.24976/Discov.Med.202537202.232

FOSL1-ANKRD22 Transcriptional Axis Regulates Mitochondrial Homeostasis to Drive Colorectal Cancer

Xiaojun Zhang[1,†], Yutian Zhao[1,†], Qiaoling Xu[2,*], Shuai Li[1], Peipei Shen[1], Yu Xu[1]

[1]Department of Abdominal Tumor Radiotherapy, Jiangnan University Affiliated Hospital, 214122 Wuxi, Jiangsu, China
[2]Department of Nuclear Medicine, Jiangnan University Affiliated Hospital, 214122 Wuxi, Jiangsu, China
*Correspondence: Xuqiaoling99_hh@163.com (Qiaoling Xu)
[†]These authors contributed equally.
Submitted: 6 August 2025 Revised: 15 October 2025 Accepted: 24 October 2025 Published: 20 November 2025

Background: Colorectal cancer (CRC) is one of the highly prevalent malignancies worldwide and a leading cause of cancer-related mortality, with limited therapeutic options, particularly in advanced stages. This study investigates the role of the FOS-like antigen 1 (FOSL1)/ankyrin repeat domain 22 (ANKRD22) axis in regulating CRC through mitochondrial function.

Methods: ANKRD22 expression patterns in CRC tissues and adjacent normal tissues were analyzed using The Cancer Genome Atlas (TCGA) data. *In vitro* experiments were performed using CRC cell lines, where FOSL1 and ANKRD22 expression was manipulated via plasmid-mediated overexpression or short hairpin RNA (shRNA)-based silencing. Stemness was assessed using sphere formation assays, cloning assays, and Western blotting to profile expression of stemness-related proteins. FOSL1 binding to the *ANKRD22* promoter was validated by luciferase reporter and chromatin immunoprecipitation (ChIP) assays. Mitochondrial status was evaluated by measuring reactive oxygen species (ROS), calcium levels, and membrane potential.

Results: TCGA data and *in vitro* analyses revealed that both FOSL1 and ANKRD22 were highly expressed in CRC cells ($p < 0.05$). Overexpression of FOSL1 or ANKRD22 in CRC cells significantly enhanced cell proliferation, sphere formation capacity, clonogenic potential, and expression of stemness-related proteins ($p < 0.05$). FOSL1 directly bound to the *ANKRD22* promoter and transcriptionally upregulated its expression ($p < 0.05$). FOSL1 overexpression decreased mitochondrial ROS, calcium, and membrane potential ($p < 0.05$). Crucially, silencing ANKRD22 reversed the effects of FOSL1 overexpression on stemness (sphere formation, clonogenicity, stemness-related proteins) and mitochondrial parameters (ROS, calcium, membrane potential) ($p < 0.05$).

Conclusion: FOSL1 transcriptionally activates *ANKRD22*, which regulates mitochondrial function by controlling ROS, calcium, and membrane potential, to modulate CRC development. Targeting the FOSL1/ANKRD22 axis may represent a strategy to impede CRC progression.

Keywords: colorectal cancer; stemness; mitochondria; ankyrin repeat domain 22; FOS-like antigen 1

Introduction

By statistics, colorectal cancer (CRC) ranks third in cancer incidence and second in cancer mortality [1]. Although the 5-year survival rate for early CRC (stage I) is 91%, for patients with metastatic involvement, the survival rate drops sharply to approximately 14% [2]. The number of new CRC cases worldwide in 2020 was 56,960, with high prevalence rates recorded in Croatia and Greece [3]. In 2018, data from the Chinese Cancer Center showed that the incidence of CRC ranked fifth among male cancers and fourth among female cancers, with approximately 130,000 new cases each year [4]. Owing to the growing incidence and prevalence of CRC, more therapeutic approaches to hamper CRC progression are warranted. In particular, molecular targeted therapy stands as an effective means of CRC treatment [5,6]. By analyzing differential gene expression in GSE164191 and GSE103512 datasets from The Cancer Genome Atlas (TCGA) database, we identified four genes, namely collagen type X alpha 1 chain (*COL10A1*), ankyrin repeat domain 22 (*ANKRD22*), H3 clustered histone 3 (*HIST1H3C*), and H2A clustered histone 8 (*HIST1H2AE*). A previous study showed that the ANKRD family is related to the occurrence of cancer [7]. Therefore, ANKRD22 was selected for thorough investigation in this research. Through the hTFtarget database, we also identified FOS-like antigen 1 (FOSL1) as a transcription factor of *ANKRD22*, providing additional insights into improving the efficacy of CRC treatments by studying the regulatory relationship between ANKRD22 and FOSL1 in the CRC context.

ANKRD22 is a nuclear-encoded mitochondrial membrane protein that is highly expressed in normal gastric mucosal epithelial cells and activated macrophages [8]. ANKRD22 belongs to the ANKRD family of proteins, which plays an instrumental role in cancer development and

progression [9,10]. *ANKRD11* acts as a tumor suppressor gene in breast cancer, with its downregulation promoting breast tumorigenesis [11]. A previous study has found that ANKRD1, a transcriptional repressor of the androgen receptor, is downregulated by testosterone and can enhance the proliferation of renal cancer cells [12]. ANKRD12 exhibits a low expression in CRC tumors, correlating with liver metastasis and reduced survival rates in CRC patients [13]. However, the mechanistic role of ANKRD22 in CRC remains uncertain.

As a mitochondrial membrane protein, the expression of ANKRD22 is related to mitochondrial function; the knockdown of ANKRD22 also reduced mitochondrial membrane potential [14]. It cooperates with lipid transporter extended synaptotagmin-1 (E-syt1) to mediate lipid transport to mitochondria, thereby reducing mitochondrial number and promoting metabolic reprogramming [15]. Mitochondria are central to metabolic reprogramming in tumor cells [15]. Several studies have shown that mitochondria in stem cells are fewer in number, less metabolically active, and more mature [16]. Researchers have discovered that inhibiting cancer cell stemness provides a potential strategy for treating osteosarcoma [17]. Cancer cells can alter how they generate energy by shifting from mitochondrial oxidative phosphorylation to glycolysis [18]. Moreover, the upregulation of calcium levels in cancer stem cells can lead to mitochondrial dysfunction [19]. At present, there are very few studies on the role of ANKRD22 in the mitochondrial metabolic reprogramming of CRC. Therefore, more investigations are needed to explore the relationship between ANKRD22 and mitochondria in CRC cells and to delineate the association between ANKRD22 and CRC cell stemness.

Based on the TCGA data, expression of both FOSL1 and ANKRD22 is upregulated in CRC. FOSL1 is involved in transcribing the oncogenic factor enolase 2 (ENO2) in *BRAF* V600E-mutated CRC [20] and has been implicated in cancer stem cell reprogramming, though specific mechanisms require clarification [21]. Based on these associations, we hypothesize that FOSL1 may transcriptionally regulate *ANKRD22*, thereby modulating mitochondrial homeostasis and potentially influencing CRC cell stemness—processes that warrant further investigation.

Materials and Methods

TCGA Database Analysis

The expression levels of ANKRD22 and FOSL1 in CRC tissues ($n = 286$) and normal tissues ($n = 41$) were investigated using the TCGA database (https://www.genome.gov/Funded-Programs-Projects/Cancer-Genome-Atlas).

Cell Culture

Normal human colonic epithelial cells NCM460 (SNL-519) were purchased from Sunncell (Wuhan, China). CRC cell lines LoVo (CCL-229), HCT116 (CRL-3487), SW480 (CCL-228), SW620 (CCL-227), and DLD-1 (CCL-221) were purchased from American Type Culture Collection (Manassas, VI, USA). The cells were cultured in RPMI-1640 (11875176, Thermo Fisher, Waltham, MA, USA) containing 10% fetal bovine serum (10100147, Thermo Fisher, Waltham, MA, USA) in an incubator set at 37 °C and 5% CO_2. Identity of all cell lines was authenticated using the short tandem repeat (STR) testing, and all of them tested negative for mycoplasma contamination.

Transfection

ANKRD22 (G103353) and FOSL1 (G108869) overexpression plasmids and their negative control (NC; pDONR223 vector) were obtained from Youbio (Chongqing, China). The sequences of ANKRD22, FOSL1 and NC are shown in **Supplementary file 1**. To achieve downregulation of ANKRD22 and FOSL1, the sequences of ANKRD22 and FOSL1 were synthesized and subcloned into pRP [shRNA]-EGFP-U6>hANKRD22 and pRP [shRNA]-EGFP-U6>hFOSL1 vectors. The plasmids were constructed by VectorBuilder (Yunzhou Biotechnology (Guangzhou) Co., Ltd, Guangzhou, China). The sequences of short hairpin RNAs (shRNAs) are as follows: shANKRD22, 5′-GAGCCCATCTGCCAAGCAGCC-3′. Upon reaching 80% confluence, the cells were cultured overnight in RPMI-1640 medium. Next, solutions A and B were prepared and mixed thoroughly and evenly (A: 2.5 µg plasmid + 250 µg Opti-Minimal Essential Medium (MEM) [31985062, Thermo Fisher, Waltham, MA, USA] + 5 µL P3000 reagent [for improving transfection efficiency; L3000015, Thermo Fisher, Waltham, MA, USA]; B: 5 µL Lipofectamine 3000 reagent diluted in 250 µg Opti-MEM medium). The solutions were allowed to stand at room temperature for 10 min before being added to the cells. Meanwhile, the NC (Ecoli [VB010000-9288rhy]) and shRNA negative control (shNC; Ecoli (VB010000-9339cqh)-P; sequence 5′-CCTAAGGTTAAGTCGCCCTCG-3′), which were all obtained from Yunzhou Biotechnology (Guangzhou) Co., Ltd (Guangzhou, China), were transfected.

Quantitative Real-Time Polymerase Chain Reaction (qRT-PCR)

Total RNA was obtained from the cells using the TRIzol reagent (AM9775, Invitrogen, Carlsbad, CA, USA), and reverse transcription was performed using a complementary Deoxyribonucleic Acid (cDNA) synthesis kit (11750350, Thermo Fisher, Waltham, MA, USA). Fast SYBR Green Master Mix (4385610, Thermo Fischer, Waltham, MA, USA) was utilized to conduct qRT-PCR. The PCR conditions are as follows: pre-denaturation (94 °C, 2 min, 1 cycle), denaturation (94 °C, 15 s, 40 cycles), annealing and extension (1 min). Glyceraldehyde 3-phosphate dehydrogenase 1 (GAPDH) acted as an internal reference. The rel-

Table 1. Primer sequences for qRT-PCR.

Genes	Forward primers (5′–3′)	Reverse primers (5′–3′)
ANKRD22	AGGGCATGTGAGAATCGTTTC	GTAGCATTCGTACAAGAGCCTC
FOSL1	CAGGCGGAGACTGACAAACTG	TCCTTCCGGGATTTTGCAGAT
GAPDH	CGAGATCCCTCCAAAATCAA	TGTGGTCATGAGTCCTTCCA

qRT-PCR, Quantitative Real-Time Polymerase Chain Reaction; *ANKRD22*, ankyrin repeat domain 22; *FOSL1*, FOS-like antigen 1; *GAPDH*, Glyceraldehyde 3-phosphate dehydrogenase 1.

ative expression levels were estimated by using the $2^{-\Delta\Delta Ct}$ method [22]. Each sample was tested thrice. Table 1 displays the sequences of the primers used.

Clonogenic and Sphere Formation Assays

LoVo and HCT116 cells, with a cell density of 4 $\times$ 10^3 each, were trypsinized, counted, and resuspended as single-cell suspension, followed by inoculation in 6-well ultra-low attachment plates (3471, Corning, Corning, NY, USA) with Roswell Park Memorial Institute (RPMI)-1640 medium containing 20 ng/mL basic fibroblast growth factor (b-FGF; PHG0026, Thermo Fisher, Waltham, MA, USA), 2% B-27 supplement (A5047501, Thermo Fisher, Waltham, MA, USA), 20 ng/mL epidermal growth factor (EGF; PF1102, Cellregen, Beijing, China), 0.4% bovine serum albumin (BSA; BS114-500g, Biosharp, Nantong, China) and 1% N-2 supplement (17502001, Thermo Fisher, Waltham, MA, USA). After 10 days of cell culture, the sphere-forming ability of the cells was evaluated using the ImageJ software (V1.46, National Institutes of Health, Bethesda, MA, USA) by enumerating the relative number of tumorspheres. Phosphate-buffered saline (PBS; AM9624, Thermo Fisher, Waltham, MA, USA) was used to rinse the colonies, whereas 4% paraformaldehyde (I28800, Thermo Fisher, Waltham, MA, USA) was used for fixation (10 min). Next, crystal violet (1%, 1 mL/well; R40073, Thermo Fisher, Waltham, MA, USA) solution was added for staining. Finally, the cells were washed thrice with PBS, followed by drying and imaging.

Western Blotting

LoVo and HCT116 cells were lysed in RIPA buffer (20118ES60, Yeasen, Shanghai, China). Protein concentration in the collected supernatant was quantitatively analyzed using a Bicinchoninic Acid Assay (BCA) kit (20201ES76, Yeasen, Shanghai, China). After boiling (5 min) in sodium dodecyl sulfate (SDS)-loading buffer, SDS-polyacrylamide gel electrophoresis (SDS-PAGE) was conducted. The separated proteins were then transferred to a polyvinylidene fluoride membrane (PVDF; 88518, Thermo Fisher, Waltham, MA, USA). The membrane was blocked with Tris Buffered Saline with Tween 20 (TBST) containing 5% skim milk (1 h) and incubated overnight (4 °C) with primary antibodies (Abcam, Cambridge, UK) targeting homeobox transcription factor Nanog (NANOG; 1:1000; ab109250, 37 kDa), organic cation/carnitine transporter 4 (OCT4; 1:1000; ab181557, 45 kDa), sex determining region Y-box 2 (SOX2; 1:1000; ab92494, 35 kDa) and GAPDH (1:1000; ab8245; 37 kDa). These antibodies were diluted in TBST with 5% BSA. Subsequently, the membrane was incubated with secondary antibody (Abcam, Cambridge, UK): goat Anti-Rabbit IgG (1:1000; ab150077) or goat Anti-Mouse IgG (1:1000; ab150113) for 1 h at room temperature. Imaging was performed on an iBright CL750 instrument (A44116, Thermo Fisher, Waltham, MA, USA) using the Enhanced Chemiluminescence (ECL) Plus HRP Substrate Kit (k22030, abbkine, Wuhan, China). Quantitative data from the Western blot were analyzed using the ImageJ software.

Mito-Sox Staining

Levels of the mitochondrial ROS generated by LoVo and HCT116 cells were evaluated by means of Mito-Sox staining. In brief, 4 $\times$ 10^3 cells were grown in 24-well plates with glass coverslips, washed with PBS, and cultivated with 5 µM Mito-Sox (M36008, Invitrogen, Carlsbad, CA, USA) at 37 °C in the dark for 15 min. Nuclear staining was performed using 4′,6-diamidino-2-phenylindole (DAPI; C1005, Beyotime, Shanghai, China). A fluorescent microscope (FV1000, Olympus, Japan) was used to randomly photograph the sample from five different view fields. Finally, the ImageJ software was used to examine the fluorescence intensity.

Measurement of Mitochondrial Membrane Potential ($\Delta\Psi M$)

Mitochondrial membrane potential (MMP) was measured using the membrane potential kit (C2001S, Beyotime, Shanghai, China). First, the cells were washed twice with PBS and soaked in 1 mL tetramethylrhodamine (TMRE) staining solution for 30 min at 37 °C. The supernatant was discarded and the cells were washed twice with pre-warmed PBS. The culture plates were then filled with 2 mL pre-warmed cell culture medium before being observed under a microscope. The nuclei were stained using DAPI (C1005, Beyotime, Shanghai, China).

Mitochondrial Calcium Determination

To measure levels of mitochondrial calcium, Rhod-2AM (R1244, Invitrogen, Carlsbad, CA, USA) was dissolved in dimethyl sulfoxide (DMSO; D12345, Invitrogen, Carlsbad, CA, USA). Rhod-2AM was given at a final con-

centration of 3 µM. Cells were incubated with reduced Rhod-2AM (3 µM) for 20 min and washed with serum-free RPMI-1640 medium for 10 min. The dye combines with mitochondrial calcium and displays red fluorescence. Raw images were processed using the ImageJ software to analyze Rhod-2AM fluorescence. Rhod-2AM fluorescence was calculated by subtracting the background value from the total fluorescence value and displayed as a histogram. DAPI (C1005, Beyotime, Shanghai, China) was utilized for nuclear staining.

In Silico ANKRD22-FOSL1 Binding Analysis and Dual Luciferase Reporter Assay

Transcription factors of ANKRD22 were predicted using the hTFtarget database (https://guolab.wchscu.cn/hTFtarget/#!/), which identified FOSL1 as the transcription factor. For predicting the binding sites between ANKRD22 and FOSL1, an analysis tool on Jaspar (http://jaspar.genereg.net/) was utilized.

In vitro, the cells were seeded and incubated overnight in 24-well plates. The pGL3-ANKRD22 plasmid was constructed as follows: The *ANKRD22* promoter region was amplified through polymerase chain reaction (PCR) using the primer pair: 5′-GAATATCAAAATATCTGTCTCACTTCT-3′ and 5′-TTTTAAAAACAATTTATTTACAAAATAT-3′. The PCR products and the pGL3-basic vector were digested with Sac I and Xba I, and the *ANKRD22* promoter fragment (1470 bp) was inserted into pGL3-basic at identical sites, yielding the vector pGL3-ANKRD22-luc. Then, pGL3-ANKRD22-luc luciferase reporter was co-transfected with various plasmids or small interfering RNAs (siRNAs), including siNC (5′-CACUCCAGCAAUAAUUUCUUU-3′), siFOSL1 (5′-GTCGAAGGCCTTGTGAACA-3′), FOSL1 overexpression vector and NC. To monitor transfection efficiency, the pCMV-RL plasmid encoding Renilla luciferase was included. Luciferase activity was measured using the dual-glo luciferase assay (Promega, Madison, WI, USA) after transfection for 24 h.

Chromatin Immunoprecipitation Assay

Chromatin immunoprecipitation (ChIP) was performed using a commercial ChIP kit (17-371, Millipore, Boston, MA, USA). 3×10^6 cells were treated with 1% formaldehyde (EIACH2O, Thermo Fisher, Waltham, MA, USA) for 15 min prior to sonication. The sonicated lysates were centrifuged at 12,000 ×g for 10 min at 4 °C to collect the soluble chromatin supernatant. The supernatant was pretreated with 70 µL protein G agarose. Anti-FOSL1 (1:500; PA5-81175, Thermo Fisher, Waltham, MA, USA) and goat anti-rabbit IgG (1:1000; 31460, Thermo Fisher, Waltham, MA, USA) were separately used in the anti-FOSL1 and IgG groups. The samples were probed overnight with the anti-FOSL1/anti-rabbit IgG antibodies and then with 70 µL protein G agarose for 2 h. Then, each antibody/agarose complex was incubated with 200 µL elution buffer (20 min). Following a 2-minute centrifugation, the supernatant was treated with 5 M NaCl to reverse DNA-protein cross-links, and then with RNase A to remove RNA. Subsequently, the samples were exposed to reagents A, B, and C successively, and finally, the eluate was subjected to qRT-PCR detection.

Statistical Analysis

GraphPad 8.0 (GraphPad Software, San Diego, CA, USA) was employed to conduct statistical analysis, with $p < 0.05$ set as the threshold for determining statistical significance. The results are expressed as mean ± standard deviation. Comparisons between two groups were conducted using an independent samples *t*-test, whereas those involving more than two groups were performed using one-way analysis of variance (ANOVA) with Tukey's post hoc test.

Results

ANKRD22 Is Upregulated in CRC Cells and Promotes Tumor Cell Proliferation

Through bioinformatics analysis of 286 tumor samples and 41 normal tissue samples in the TCGA database, we found that ANKRD22 was markedly upregulated in CRC ($p < 0.05$, Fig. 1A). Furthermore, the expression of ANKRD22 in normal human colonic epithelial cell (NCM460) and CRC cell lines (LoVo, HCT116, SW480, SW620, DLD-1) was detected; compared with the NCM460 cells, the CRC cell lines exhibited higher expression level of ANKRD22 ($p < 0.05$, Fig. 1B). Among them, LoVo and HCT116 cell lines were chosen for more in-depth mechanistic experiments.

Through lipofection transfection, we manipulated ANKRD22 expression in LoVo and HCT116 cells for the purposes of determining ANKRD22 bioactivity. Following ANKRD22 overexpression, the *ANKRD22* mRNA level was higher in the ANKRD22 group than in the NC group ($p < 0.05$, Fig. 1C,D). Contrarily, when ANKRD22 was silenced, the *ANKRD22* mRNA level was reduced in the shANKRD22 group, as compared to the shNC group ($p < 0.05$, Fig. 1C,D). Therefore, these data indicate that the transfection was successful. The clonogenic ability of the CRC cells following transfection was evaluated by cloning assay. Our findings revealed that the ANKRD22 overexpression promoted the formation of cell clones, but the clonogenic ability of cells was weakened after the ANKRD22 expression was silenced ($p < 0.05$, Fig. 1E–G), suggesting that ANKRD22 can significantly enhance the clonality of LoVo and HCT116 cells *in vitro*.

ANKRD22 Overexpression Promotes CRC Cell Stemness

By means of the cell sphere formation assay, the impact of ANKRD22 on the stemness of CRC cells was in-

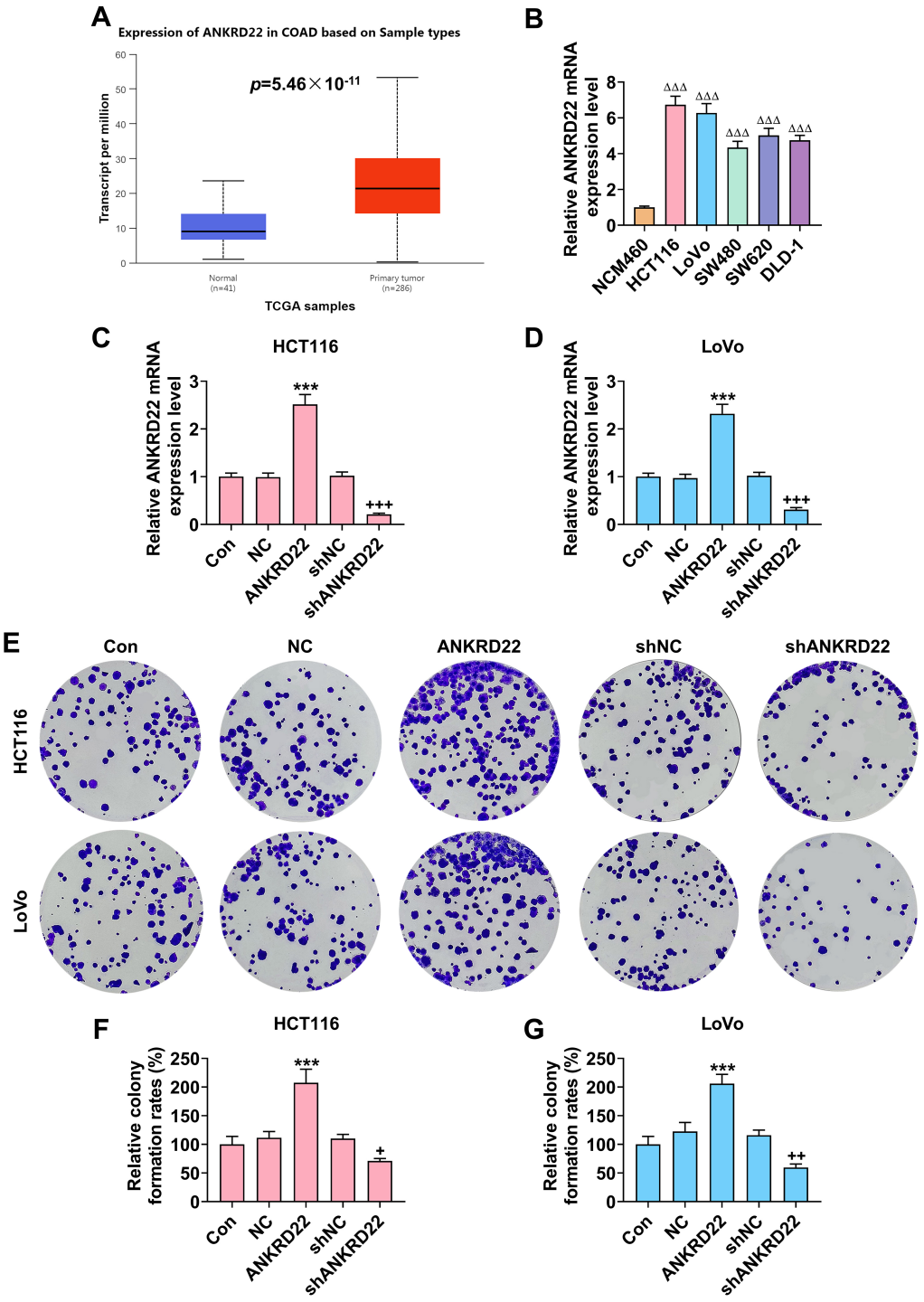

Fig. 1. ANKRD22 is upregulated in tumors based on analysis in the TCGA database. (A) ANKRD22 expression in 286 CRC tissues and 41 normal tissues (TCGA database; https://www.genome.gov/Funded-Programs-Projects/Cancer-Genome-Atlas). $p = 5.46 \times 10^{-11}$. (B) *ANKRD22* mRNA levels in normal human colonic epithelial cell (NCM460) and CRC cell lines (LoVo, HCT116, SW480, SW620, DLD-1) with *GAPDH* as an internal reference (qRT-PCR). (C,D) *ANKRD22* mRNA levels in CRC cell lines (HCT116 and LoVo) with *GAPDH* as an internal reference (qRT-PCR). (E–G) Effect of ANKRD22 on clonogenicity in both LoVo and HCT116 cells. Data are expressed as mean ± standard deviation of three independent experiments. $^{\Delta\Delta\Delta}p < 0.001$ vs. NCM460; $^{***}p < 0.001$ vs. NC; $^{+}p < 0.05$, $^{++}<0.001$, $^{+++}p < 0.001$ vs. shNC; n = 3. ANKRD22, ankyrin repeat domain 22; TCGA, The Cancer Genome Atlas; CRC, colorectal cancer; *GAPDH*, Glyceraldehyde 3-phosphate dehydrogenase 1; qRT-PCR, Quantitative Real-Time Polymerase Chain Reaction.

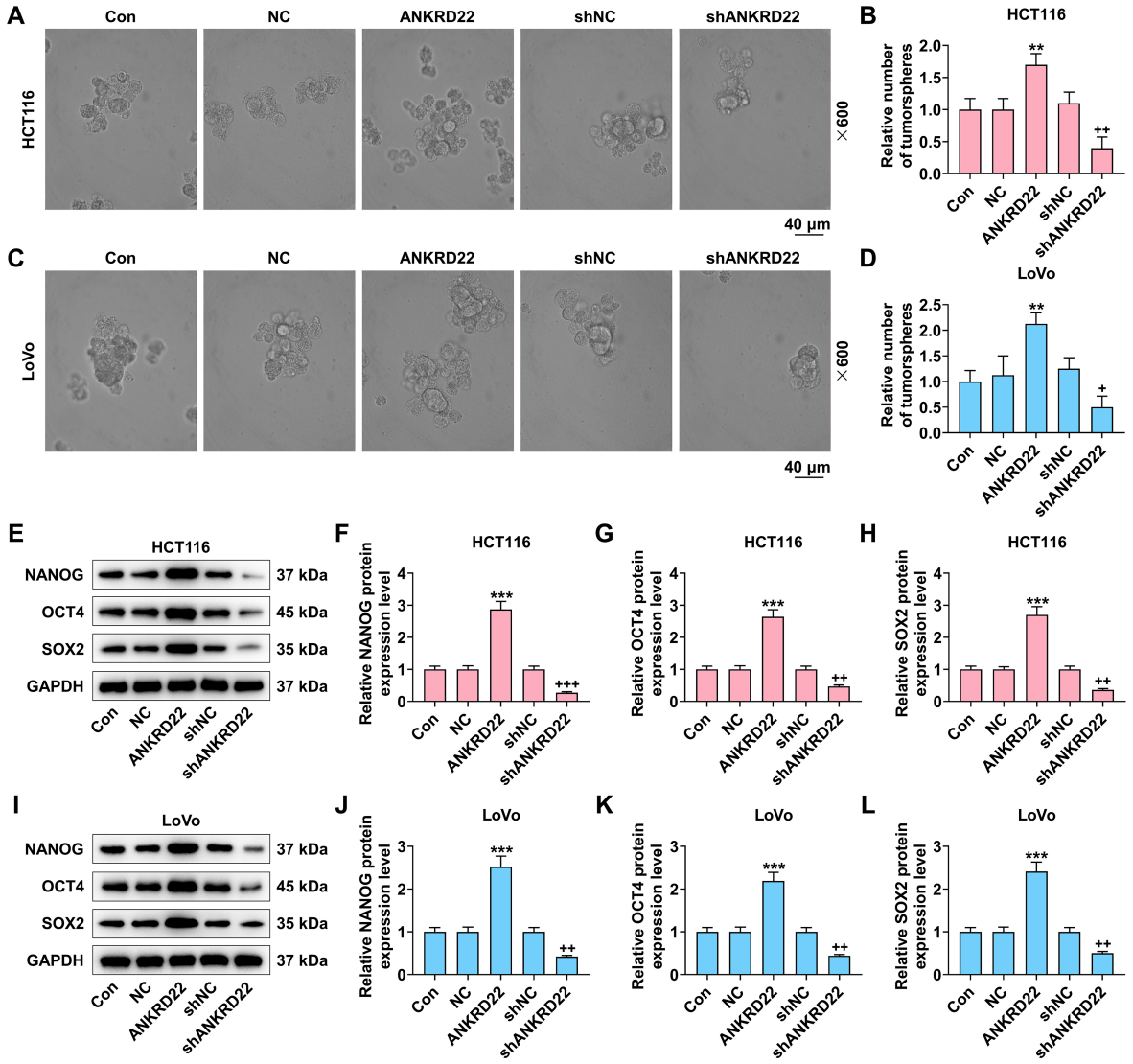

Fig. 2. ANKRD22 promotes CRC cell stemness. (A) Sphere formation in HCT116 cells. Scale bar: 40 μm; 600× magnification. (B) The relative number of tumorspheres in HCT116 cells. (C) Sphere formation of LoVo cells. Scale bar: 40 μm; 600× magnification. (D) The relative number of tumorspheres in LoVo cells. (E) Western blot results of NANOG, OCT4, and SOX2 protein levels in HCT116 cells with GAPDH as an internal reference. (F–H) Relative protein expression levels of NANOG, OCT4, and SOX2 in HCT116 cells with GAPDH as an internal reference (based on Western blot results). (I) Western blot results of NANOG, OCT4, and SOX2 protein levels in LoVo cells with GAPDH as an internal reference. (J–L) Relative protein expression levels of NANOG, OCT4, and SOX2 in LoVo cells with GAPDH as an internal reference (based on Western blot results). $^{**}p < 0.01$, $^{***}p < 0.001$ vs. NC; $^{+}p < 0.05$, $^{++}p < 0.01$, $^{+++}p < 0.001$ vs. shNC. n = 3. NANOG, homeobox transcription factor Nanog; OCT4, organic cation/carnitine transporter 4; SOX2, sex determining region Y-box 2; NC, negative control; shNC, shRNA negative control.

vestigated. Overexpression of ANKRD22 increased sphere formation and the relative number of tumorspheres, while silencing ANKRD22 in CRC cells yielded the opposite results ($p < 0.05$, Fig. 2A–D). According to results shown in Fig. 2E–H, protein levels of NANOG, OCT4 and SOX2 in HCT116 cells were all increased following ANKRD22 overexpression but exhibited a reduction when ANKRD22 was silenced ($p < 0.05$, Fig. 2E–H). Consistent results were also detected in the LoVo cells ($p < 0.05$, Fig. 2I–L).

ANKRD22 Mediates Mitochondrial Function in CRC Cells by Regulating ROS, Calcium and Membrane Potential Levels

Mitochondrial ROS levels were used as a parameter to assess mitochondrial function. A Mito-Sox kit was employed to detect mitochondrial ROS levels in the CRC cells, and the results showed that ANKRD22 overexpression suppressed mitochondrial ROS levels in HCT116 cells, whereas ANKRD22 silencing promoted ROS levels ($p <$

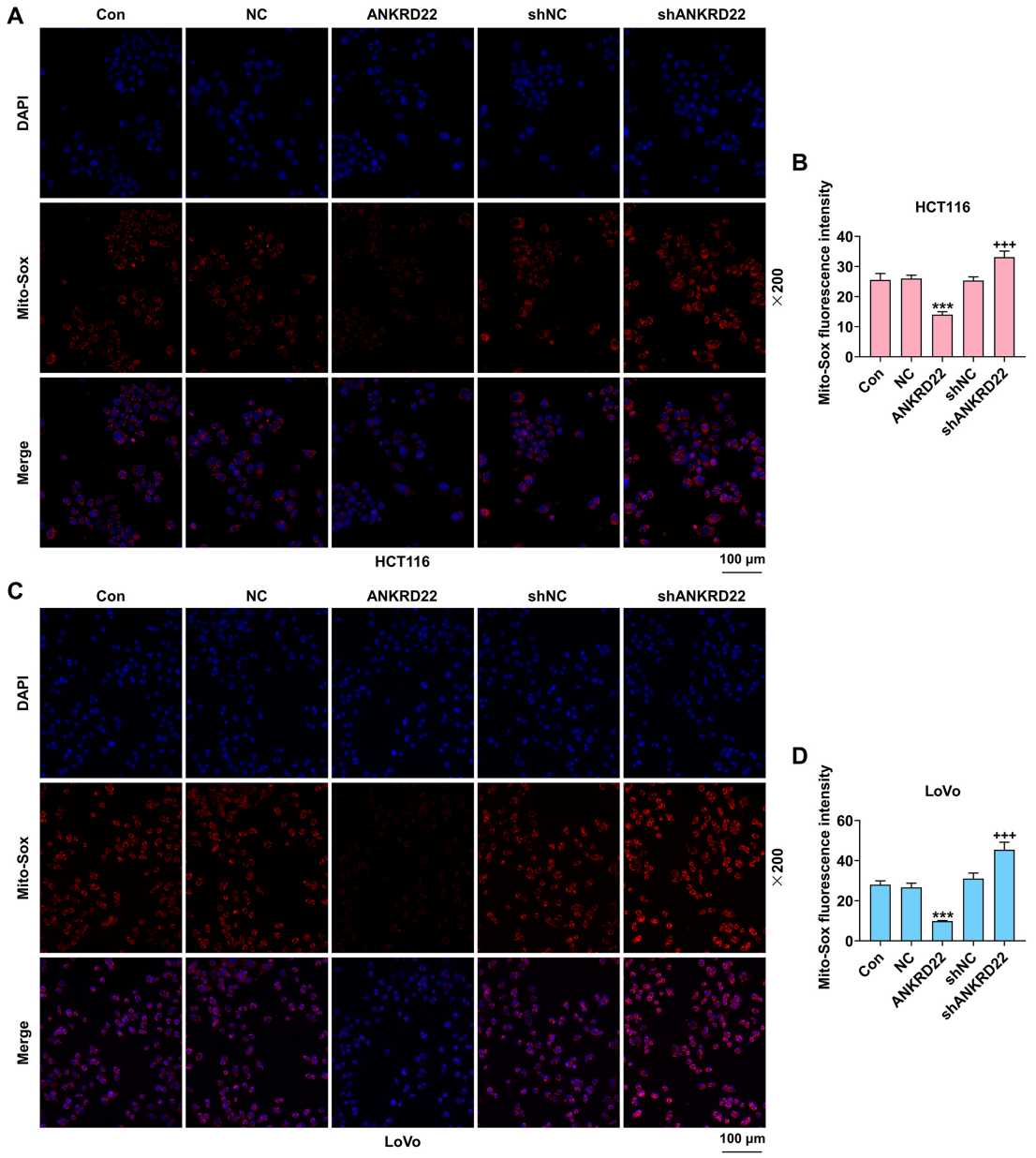

Fig. 3. ANKRD22 regulates levels of mitochondrial ROS. (A) Staining results of mitochondrial ROS in HCT116 cells. (B) Quantitative results of mitochondrial ROS in HCT116 cells. (C) Staining results of mitochondrial ROS in LoVo cells. (D) Quantitative results of mitochondrial ROS in LoVo cells. $^{***}p < 0.001$ vs. NC; $^{+++}p < 0.001$ vs. shNC. n = 3. ROS, reactive oxygen species.

0.05, Fig. 3A,B). Similar results were replicated in the context of LoVo cells ($p < 0.05$, Fig. 3C,D).

Additionally, to comprehensively understand the impact of ANKRD22 on mitochondrial function, we analyzed mitochondrial calcium levels using the Rhod-2AM probe. Our results showed that ANKRD22 could regulate the mitochondrial calcium level in HCT116 cells (Fig. 4A,B) and LoVo cells (Fig. 4C,D); the calcium level increased when ANKRD22 was silenced, and the calcium decreased when ANKRD22 was overexpressed (both $p < 0.05$). These outcomes substantiate the negative relationship of ANKRD22 level with mitochondrial ROS and calcium levels.

According to Fig. 5A–D, we observed that the silencing of ANKRD22 increased the MMP, and *vice versa* ($p < 0.05$), indicating that ANKRD22 promoted the survival of CRC cells by decreasing ROS, calcium, and MMP.

ANKRD22 Is Transcriptionally Regulated by FOSL1 In Vitro

Based on the TCGA database analysis, FOSL1 was upregulated in CRC tissues ($p < 0.05$, Fig. 6A). Analysis with JASPAR revealed that there were binding sites between FOSL1 and ANKRD22 (Fig. 6B). qRT-PCR analysis revealed downregulated FOSL1 expression after silenc-

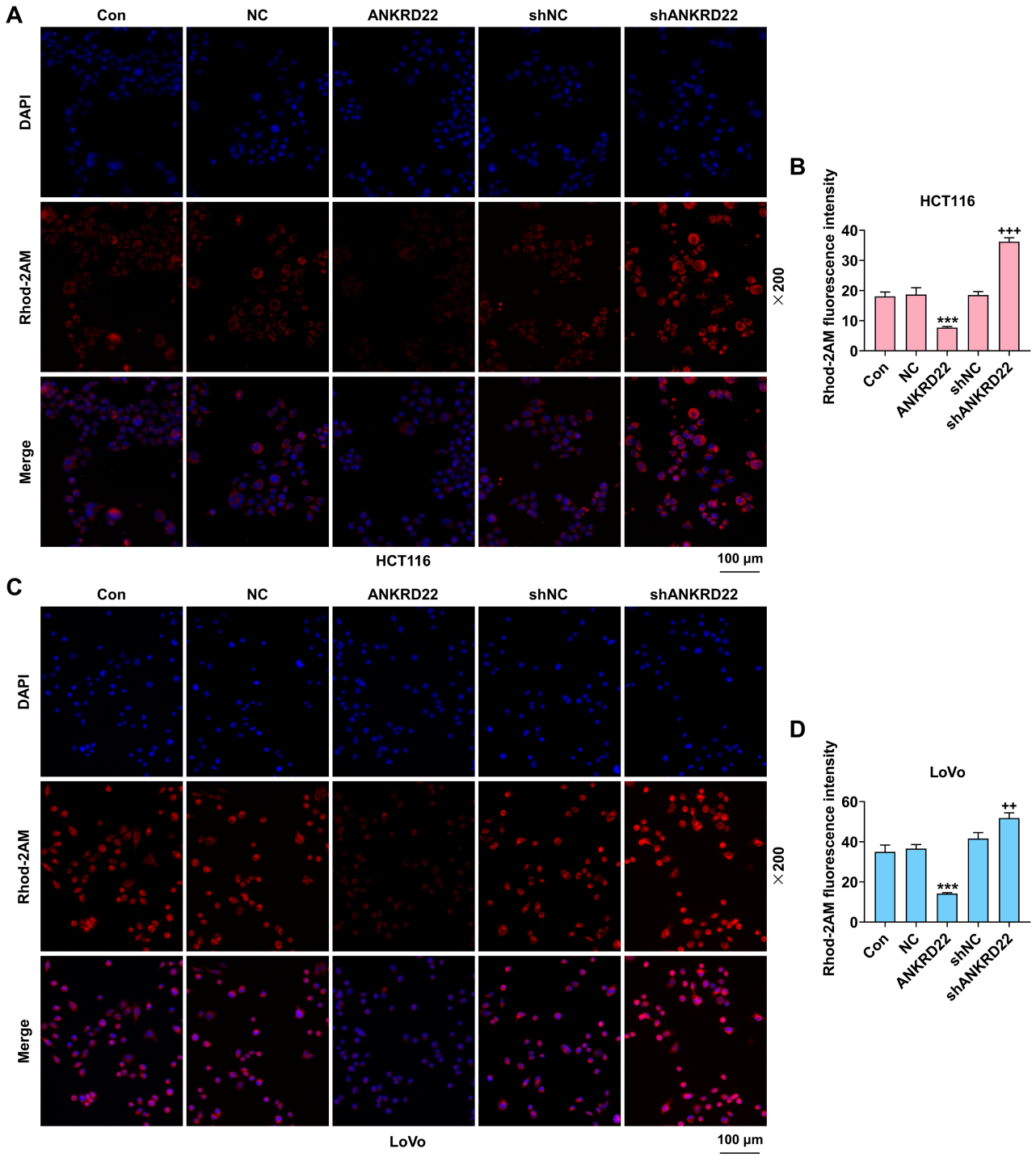

Fig. 4. ANKRD22 regulates levels of mitochondrial calcium. (A) Staining results of mitochondrial calcium in HCT116 cells. (B) Quantitative results of mitochondrial calcium in HCT116 cells. (C) Staining results of mitochondrial calcium in LoVo cells. (D) Quantitative results of mitochondrial calcium in LoVo cells. $^{***}p < 0.001$ vs. NC; $^{++}p < 0.01$, $^{+++}p < 0.001$ vs. ShNC. n = 3.

ing, indicating successful transfection ($p < 0.05$, Fig. 6C). To validate the binding interaction between FOSL1 and ANKRD22, a dual luciferase reporter assay was conducted. We discovered that luciferase activity of the *ANKRD22* promoter decreased by approximately 60% when FOSL1 expression was reduced and increased by approximately 50% following FOSL1 overexpression in the CRC cells ($p < 0.05$, Fig. 6D). These findings suggest that FOSL1 binds to the *ANKRD22* promoter. Next, the binding relation of FOSL1 to *the ANKRD22* promoter in the CRC cells was further investigated using a ChIP assay. Our results showed that, when compared to mock precipitation, the enrichment

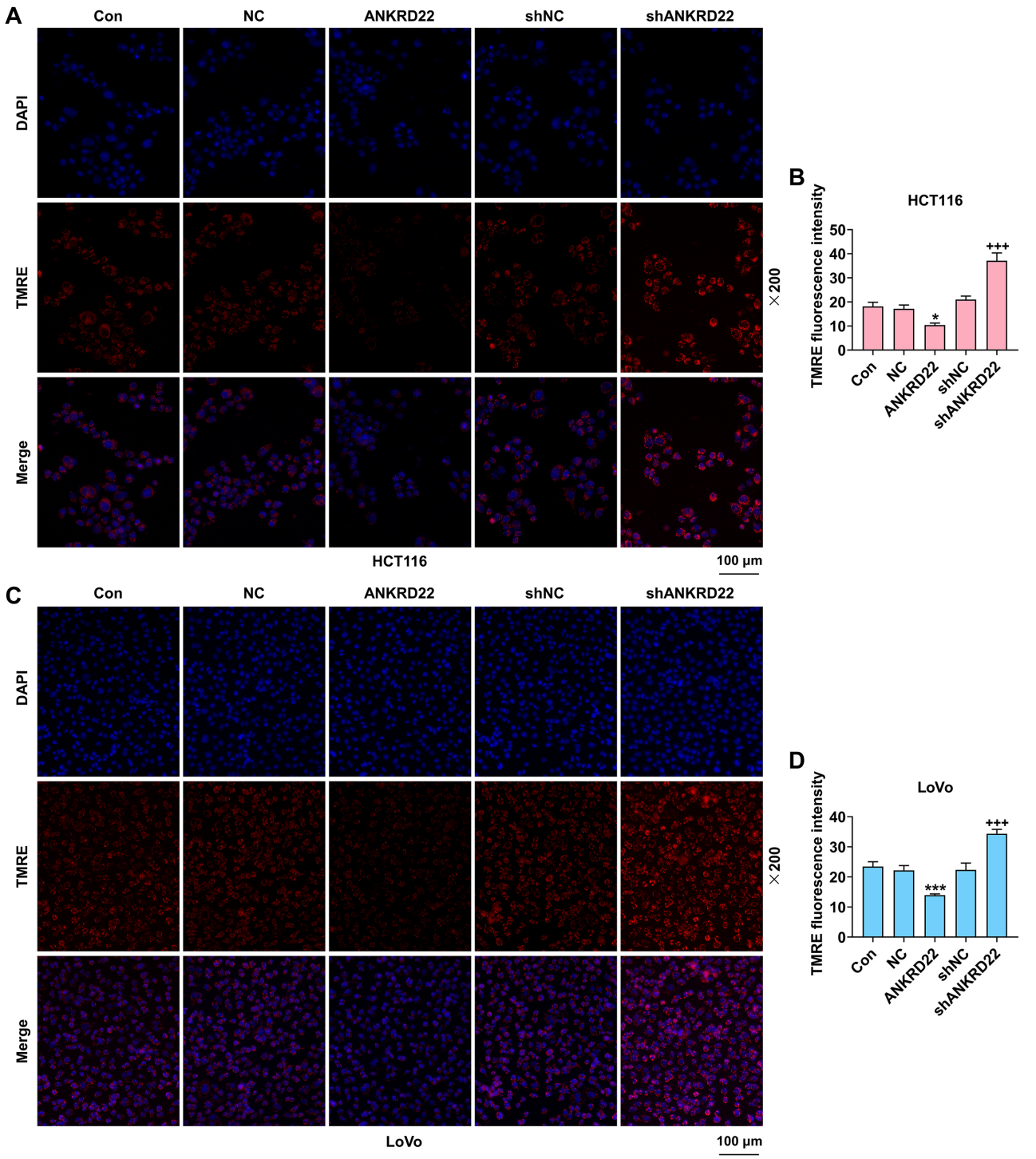

Fig. 5. ANKRD22 modulates mitochondrial membrane potential. (A) TMRE fluorescence staining results in HCT116 cells. (B) Quantitative results of TMRE fluorescence intensity in HCT116 cells. (C) TMRE fluorescence staining results in LoVo cells. (D) Quantitative results of TMRE fluorescence intensity in LoVo cells. $^{*}p < 0.05$, $^{***}p < 0.001$ vs. NC; $^{+++}p < 0.001$ vs. shNC. n = 3. TMRE, tetramethylrhodamine.

degree was elevated in the anti-FOSL1 group ($p < 0.05$, Fig. 6E), suggesting that FOSL1 bound to the ANKRD22 promoter *in vitro*. Thus, this result indicates that FOSL1 binds to the ANKRD22 promoter and regulates its activity, ultimately mediating ANKRD22 expression.

To unravel the regulatory role of the FOSL1 in mediating ANKRD22 expression and activity *in vitro*, we first verified the function of FOSL. A qRT-PCR assay was conducted to assess the transfection efficiency of FOSL1 vectors. Overexpression of FOSL1 resulted in a 2.2-fold in-

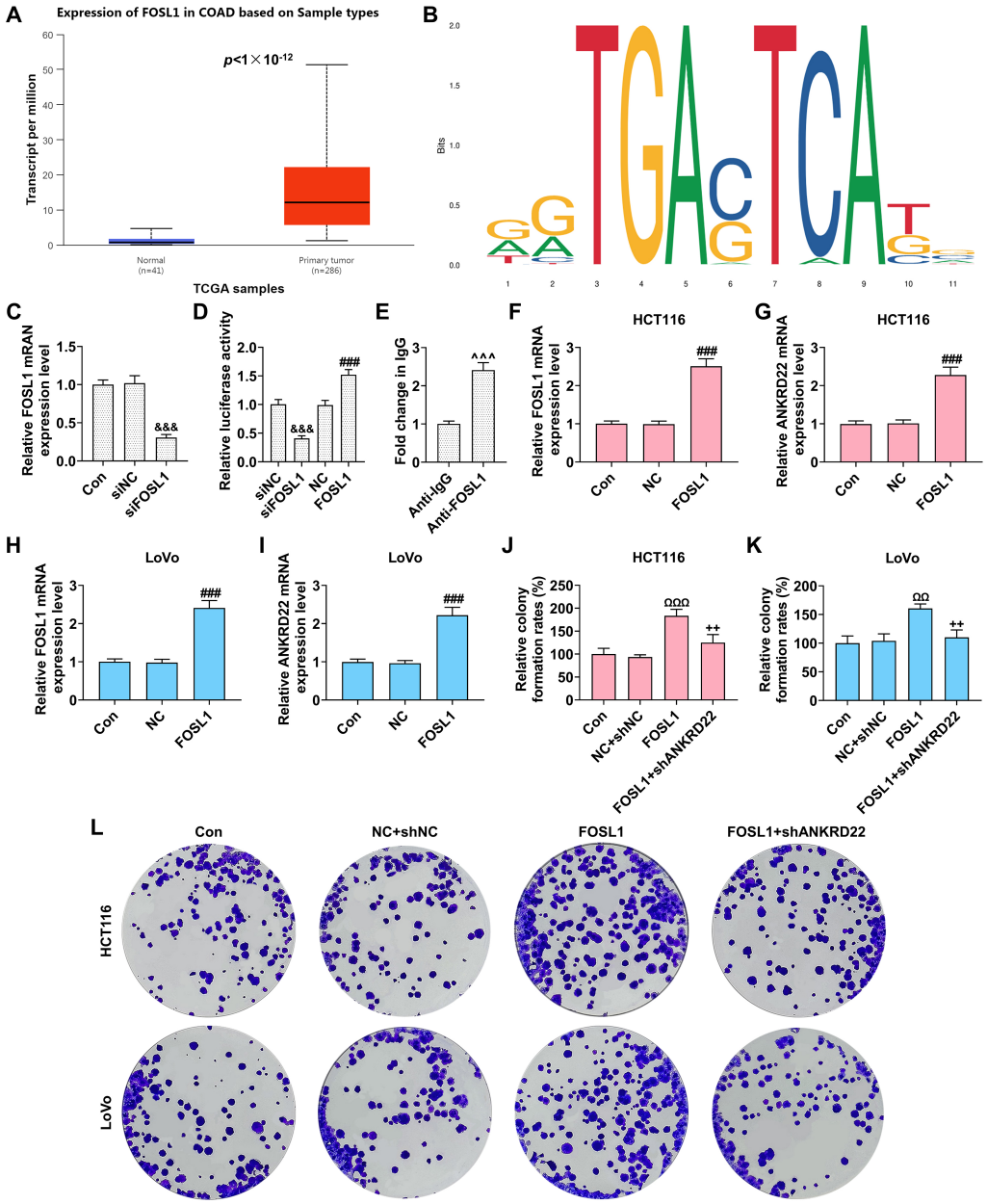

Fig. 6. ANKRD22 is transcriptionally regulated by FOSL1 *in vitro*. (A) Analysis of FOSL1 expression in 286 CRC tissues and 41 normal tissues (TCGA database; https://www.genome.gov/Funded-Programs-Projects/Cancer-Genome-Atlas). Expression of FOSL1 was upregulated in tumor tissues ($p < 1 \times 10^{-12}$). (B) Identification of binding sites for FOSL1 on the *ANKRD22* promoter using the JASPAR analysis tool. (C) The expression of *FOSL1* was detected by qRT-PCR to evaluate transfection efficacy. (D) Results of luciferase reporter assay for validating the binding relationship between the FOSL1 and the *ANKRD22* promoter region. (E) ChIP results showing FOSL1 binding to the *ANKRD22* promoter. (F) Relative mRNA expression level of *FOSL1* in HCT116 cells (qRT-PCR). (G) Relative mRNA expression level of *ANKRD22* in HCT116 cells (qRT-PCR). (H) Relative mRNA expression level of *FOSL1* in LoVo cells (qRT-PCR). (I) Relative mRNA expression level of *ANKRD22* in LoVo cells (qRT-PCR). *GAPDH* was used as an internal reference in all qRT-PCR assays. (J) Relative colony formation rates in HCT116 cells. (K) Relative colony formation rates in LoVo cells. (L) Effect of FOSL1 overexpression on clonogenicity in HCT116 and LoVo cells. $^{###}p < 0.001$ vs. siNC; $^{\wedge\wedge\wedge}p < 0.001$ vs. anti-IgG; $^{\Omega\Omega}p < 0.01$, $^{\Omega\Omega\Omega}p < 0.001$ vs. NC+shNC; $^{\&\&\&}p < 0.001$ vs. NC; $^{++}p < 0.01$ vs. shNC. n = 3. *FOSL1*, FOS-like antigen 1; ChIP, chromatin immunoprecipitation.

crease in its mRNA level (Fig. 6F) and an approximately 2.2-fold increase in the *ANKRD22* mRNA level (Fig. 6G) compared with the NC group (both $p < 0.05$). Similar alteration trends for *FOSL1* and *ANKRD22* mRNA expres-

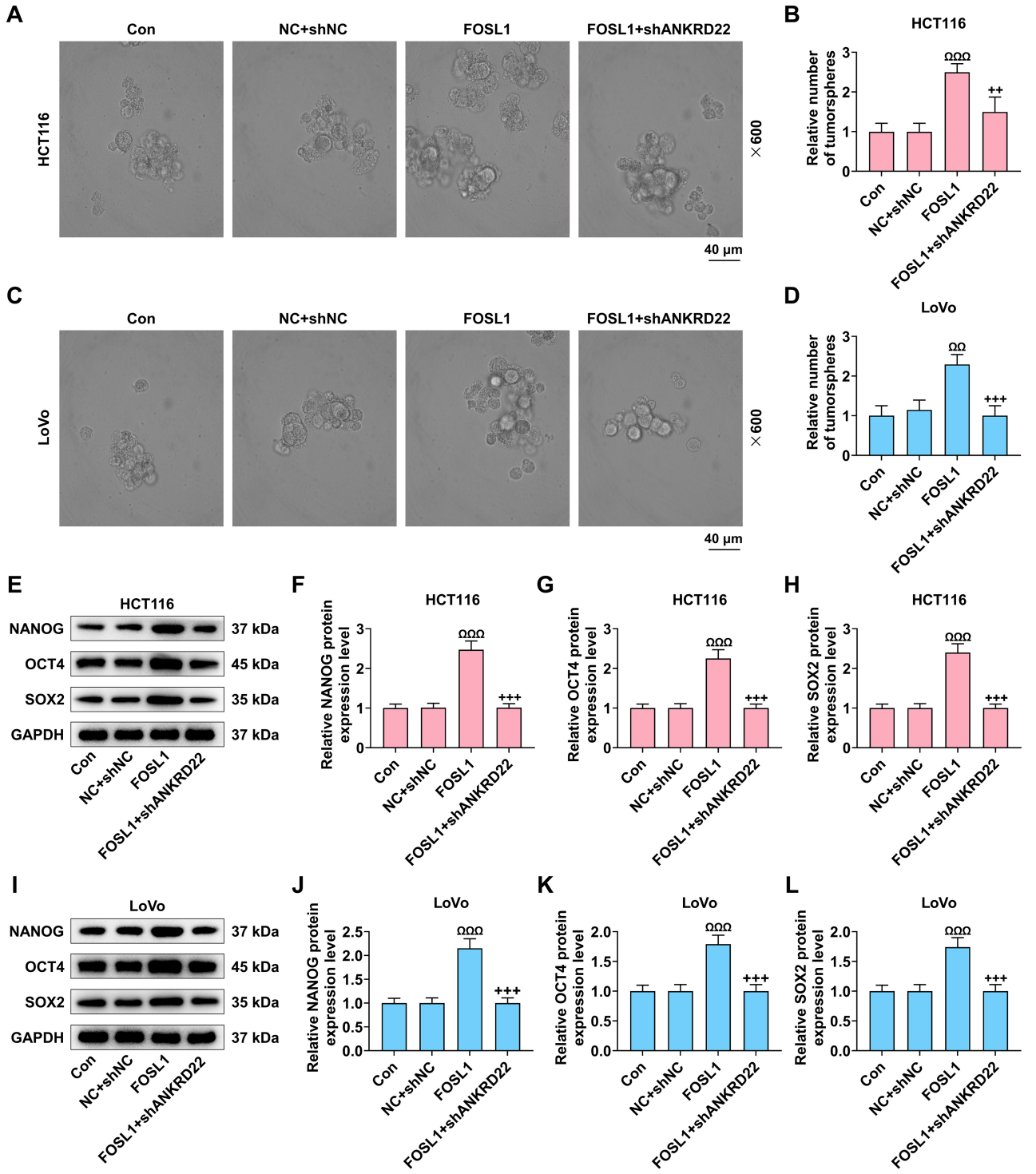

Fig. 7. FOSL1 promotes CRC cell stemness. (A) Sphere formation in HCT116 cells. Scale bar: 40 μm; 600× magnification. (B) Quantitative analysis of the relative number of tumorspheres in HCT116 cells. (C) Sphere formation in LoVo cells. Scale bar: 40 μm; 600× magnification. (D) Quantitative analysis of the relative number of tumorspheres in LoVo cells. (E) Western blot results of NANOG, OCT4, and SOX2 protein levels in HCT116 cells. (F–H) Quantitative analysis of the relative protein expression levels of NANOG, OCT4, and SOX2 in HCT116 cells (based on Western blot results). (I) Western blot results of NANOG, OCT4, and SOX2 protein levels in LoVo cells. (J–L) Quantitative analysis of the relative protein expression levels of NANOG, OCT4, and SOX2 in LoVo cells (based on Western blot results). GAPDH was used as an internal reference in all Western blotting assays. $^{\Omega\Omega}p < 0.01$, $^{\Omega\Omega\Omega}p < 0.001$ vs. NC+shNC; $^{++}p < 0.01$, $^{+++}p < 0.001$ vs. FOSL1. n = 3.

sion levels were also observed in the LoVo cells ($p < 0.05$, Fig. 6H,I). Apart from proving that the vectors had been successfully transfected, these data also depict that the *ANKRD22* mRNA level in the CRC cells is positively regulated by FOSL1. To verify the positive regulatory effect of FOSL1 on ANKRD22, we examined the clonogenic ability and colony formation rates of CRC cells. Overexpression of FOSL1 could promote HCT116 cell clonogenicity and their relative formation rates, whereas silencing ANKRD22 repressed their clonogenic ability ($p < 0.05$, Fig. 6J,L). We also observed consistent results in LoVo cells ($p < 0.05$, Fig. 6K,L). Altogether, these outcomes confirm that FOSL1 promotes clonogenicity of CRC cells *in vitro*, which is reversible with ANKRD22 silencing.

FOSL1 Regulates ANKRD22-Mediated Mitochondrial Function to Promote CRC Cell Stemness

Through the sphere formation assay, the impact of FOSL1 expression on sphere formation in CRC cells was clarified. According to Fig. 7A,B, although FOSL1 overexpression engendered the highest sphere-forming capacity in the CRC cells, this ability was significantly suppressed upon ANKRD22 silencing ($p < 0.05$). Similar experimental results were also replicated in the context of LoVo cells ($p < 0.05$, Fig. 7C,D). Collectively, these data suggest that FOSL1 promotes sphere formation in CRC cells, which can be reversed by ANKRD22 silencing.

Levels of cell stemness-related proteins were quantified by means of Western blotting. We found that NANOG, OCT4, and SOX2 protein levels were upregulated when FOSL1 was overexpressed. However, ANKRD22 silencing reduced the expression levels of these proteins ($p < 0.05$, Fig. 7E–L), implying that the role of FOSL1 in promoting cell stemness was reversible through ANKRD22 silencing. To investigate the effect of FOSL1 on mitochondrial function, we assessed mitochondrial levels of ROS, calcium, and MMP. When FOSL1 was overexpressed, the mitochondrial ROS level was reduced, but ANKRD22 silencing upregulated the mitochondrial ROS level ($p < 0.05$; Fig. 8A–D). Meanwhile, the mitochondrial calcium levels and MMP were repressed by FOSL1 overexpression but increased upon ANKRD22 silencing ($p < 0.05$; Figs. 9,10). These results indicate that FOSL1 plays an inhibitory role in the regulation of CRC cell stemness and alters mitochondrial function through the modulation of ROS, calcium, and MMP, via transcriptional regulation of ANKRD22, with ANKRD22 silencing reversing both effects, consistent with concurrent changes in mitochondrial traits and stemness markers; however, the direct mechanistic link between these processes warrants further investigation.

Discussion

ANKRD22 has previously been proposed as a marker for glioma, pancreatic cancer, and non-small cell lung cancer [23–25], but little is known about its biological role in CRC. Thus, further clarifying the molecular role of ANKRD22 in the pathogenesis and progression of CRC is particularly important for enhancing therapeutic efficacy. To explore the underlying mechanism, we employed a preliminary approach to examine the expression of ANKRD22 through the TCGA database; our *in-silico* findings revealed that the CRC tissues harbor a higher ANKRD22 expression than the normal tissues. Besides, ANKRD22 overexpression promoted cell cloning and sphere-forming ability, and enhanced expression of cell stemness-related proteins such as NANOG, OCT4, and SOX2, among which SOX2 is identified as a key factor in cell stemness [26]. Other studies also discovered that NANOG expression is associated with advanced cancer and liver metastasis in CRC patients [27], and that high OCT4 expression is an independent predictor of liver metastasis in CRC patients [28]. It has been previously reported that SOX2 expression is associated with increased CRC metastasis [29]. Collectively, these findings point to an indirect role of ANKRD22, which may regulate proliferation and stemness of CRC cells. This postulation has been validated in another study focusing on the role of ANKRD22 in breast cancer, which is, the upregulation of ANKRD22 in breast cancer promotes the metastasis and proliferation of cancer cells [15].

A growing line of evidence suggests associations between mitochondrial traits and stemness, with mitochondrial function linked to cancer stem cell properties like migration and drug resistance [30]. Mitochondria represent a primary source of intracellular ROS, and elevated levels of ROS can prevent tumor growth by continuously enhancing cell cycle inhibition [31]. Our results showed that ANKRD22 inhibited mitochondrial ROS generation in CRC cells. Separately, it has been reported that by suppressing a mitochondrial calcium overload, cancer cells can escape from apoptosis, thereby ensuring their continued survival and proliferation [32].

FOSL1 is a target gene of the β-catenin/Wnt signaling pathway that is activated following the Wnt signaling induction [33]. ANKRD22 promotes malignancy by activating the Wnt/β-catenin pathway in breast cancer [15]. Our dual luciferase reporter assay experiment confirmed that FOSL1 is a transcription factor of *ANKRD22*. By manipulating the expression of these targets, we observed that FOSL1 overexpression promoted stemness and proliferation of the CRC cells, which were reversed upon ANKRD22 silencing. Thus, we speculate that CRC cell stemness is regulated by FOSL1, with Wnt/β-catenin pathway activation acting as the trigger. In fact, activation of the Wnt/β-catenin pathway promotes cell stemness in CRC [34]. β-catenin is involved in the activation of the

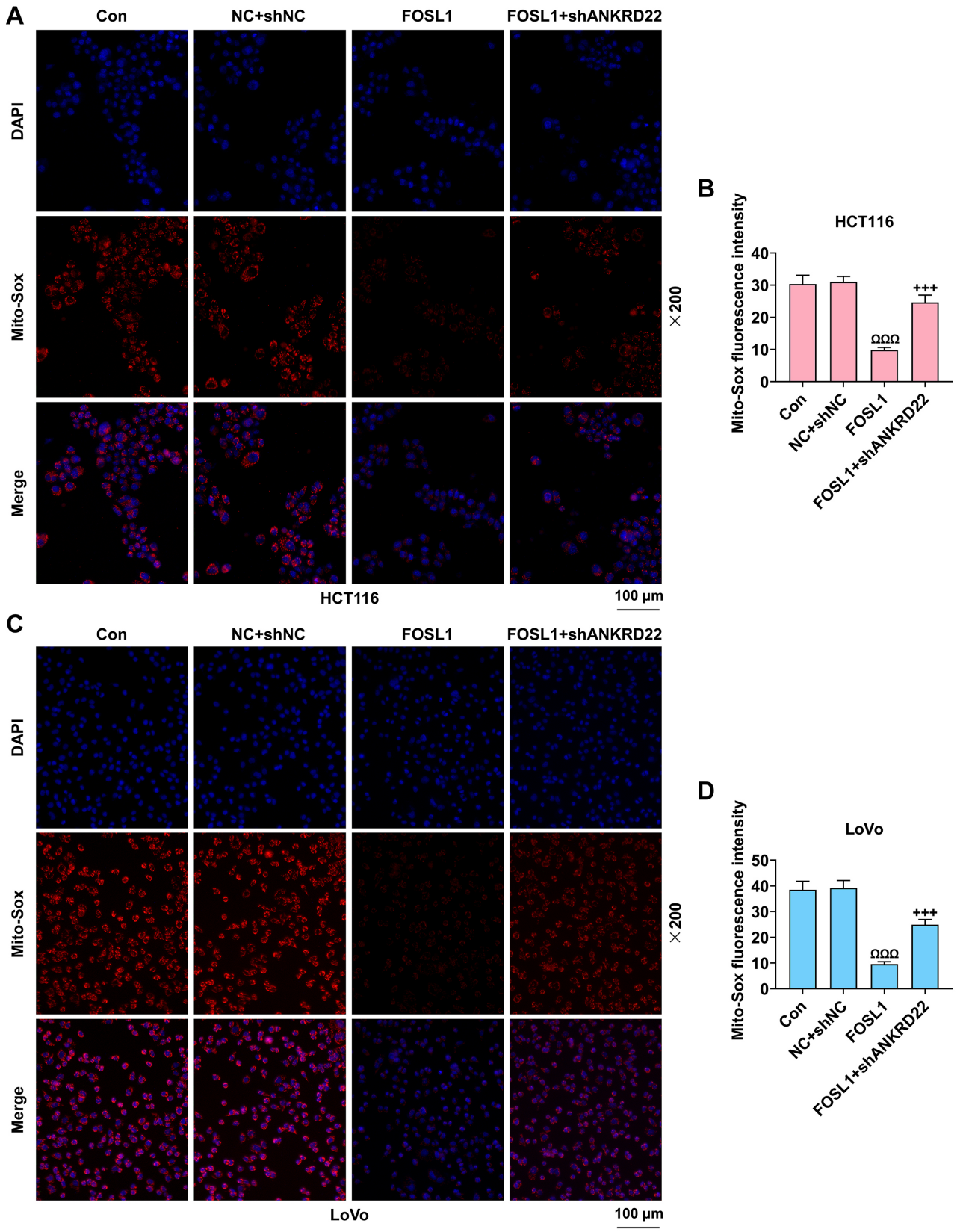

Fig. 8. FOSL1 increases mitochondrial ROS levels in CRC cells. (A) Staining results of mitochondrial ROS in HCT116 cells. (B) Quantitative results of mitochondrial ROS levels in HCT116 cells. (C) Staining results of mitochondrial ROS in LoVo cells. (D) Quantitative results of mitochondrial ROS levels in LoVo cells. $^{\Omega\Omega\Omega}p < 0.001$ vs. NC+shNC; $^{+++}p < 0.001$ vs. FOSL1. n = 3.

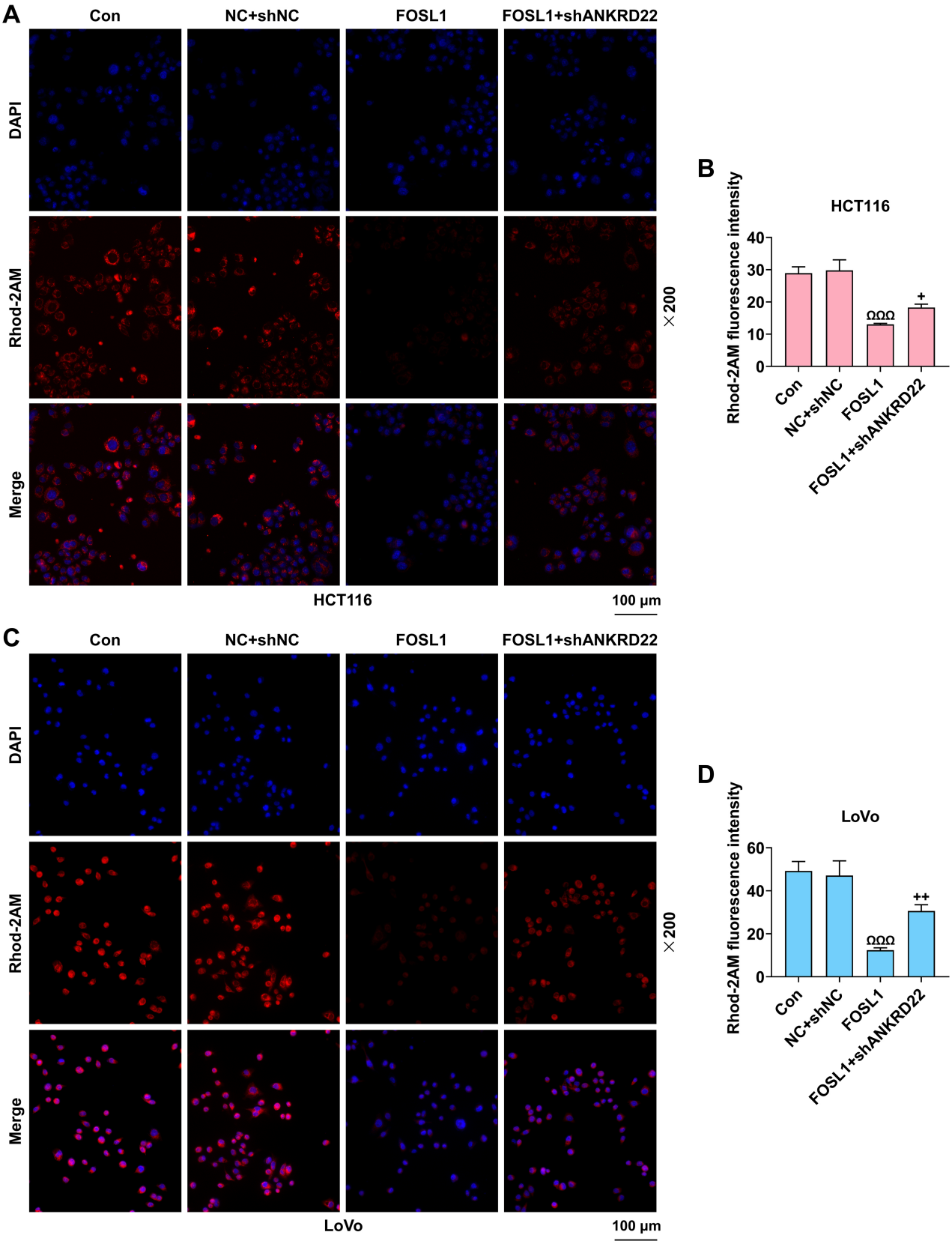

Fig. 9. FOSL1 increases calcium levels in CRC cells. (A) Staining results of mitochondrial calcium in HCT116 cells. (B) Quantitative results of mitochondrial calcium levels in HCT116 cells. (C) Staining results of mitochondrial calcium in LoVo cells. (D) Quantitative results of mitochondrial calcium levels in LoVo cells. $^{\Omega\Omega\Omega}p < 0.001$ vs. NC+shNC; $^{+}p < 0.05$, $^{++}p < 0.01$ vs. FOSL1. n = 3.

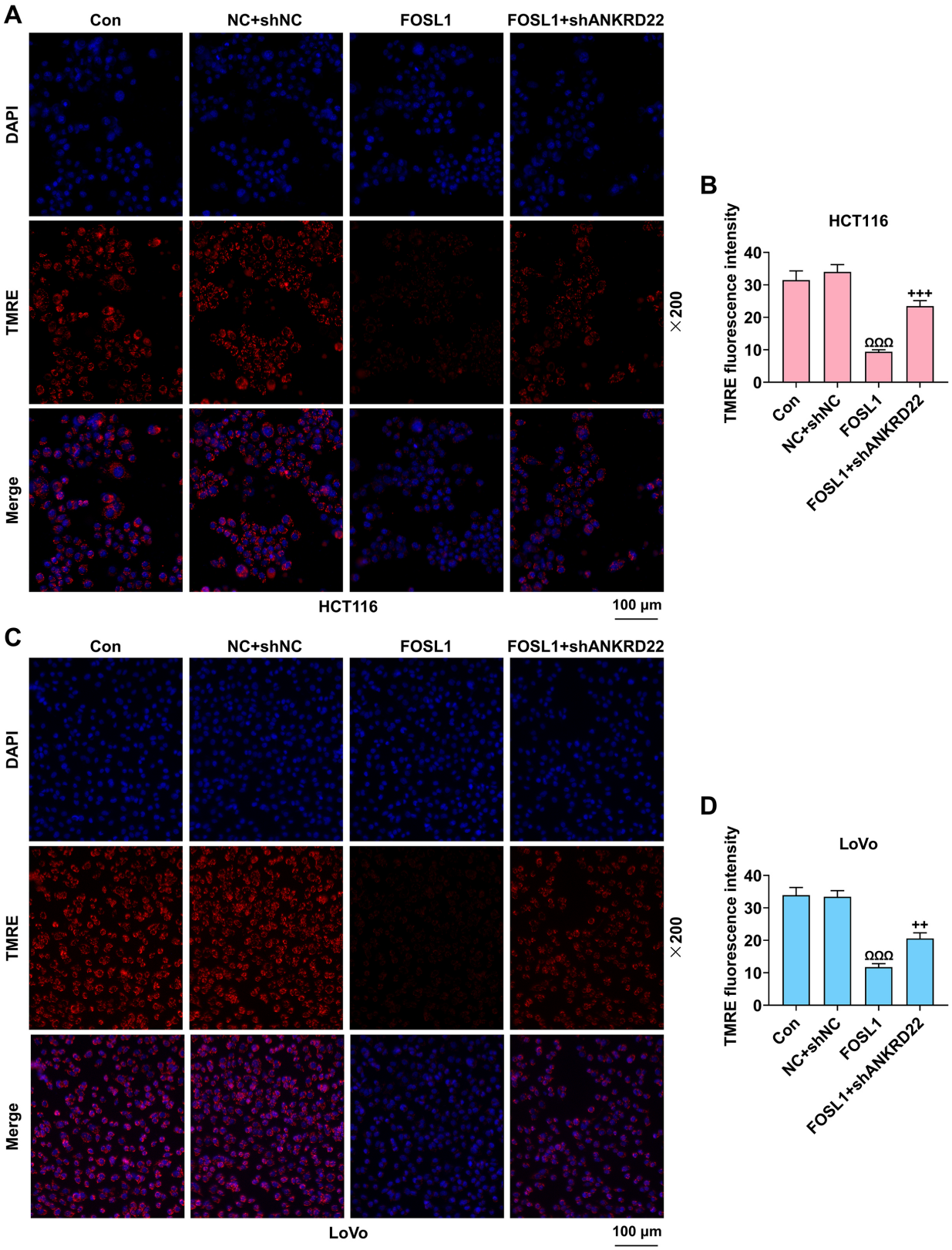

Fig. 10. FOSL1 increases MMP in CRC cells. (A) TMRE fluorescence staining results in HCT116 cells. (B) Quantitative results of TMRE fluorescence intensity in HCT116 cells. (C) TMRE fluorescence staining results in LoVo cells. (D) Quantitative results of TMRE fluorescence intensity in LoVo cells. $^{\Omega\Omega\Omega}p < 0.001$ vs. NC+shNC; $^{++}p < 0.01$,$^{+++}p < 0.001$ vs. FOSL1. n = 3.

Wnt/β-catenin signaling pathway [35], and oxidative stress within mitochondria has been shown to modulate β-catenin activity [36]. Nevertheless, this study solely investigated mitochondrial ROS without assessing the overarching oxidative stress status within the mitochondria. To comprehensively understand the correlations between FOSL1 and the Wnt/β-catenin signaling pathway, future research directions should include investigating the impacts of applying pathway inhibitors, as this will provide useful insights into retarding the CRC progression.

There are some limitations in this study. Firstly, only the commercial, established cell lines were utilized across all functional experiments in this study; however, such controlled and comparable model systems do not reflect the genetic diversity and complexity of tumors in human patients. Furthermore, our conjectures in the current study were primarily tested using only the *in vitro* models. In order to expand our knowledge along this line of research, *in vivo* investigations are warranted to unravel the physiological relevance of the findings obtained.

Conclusion

In conclusion, high levels of ANKRD22 and FOSL1 are linked to stemness and mitochondrial dysfunction in CRC cells. ANKRD22 is transcriptionally regulated by FOSL1 *in vitro*, and ANKRD22 silencing reverses FOSL1's effects on CRC cell stemness and proliferation. Thus, these findings highlight that FOSL1's transcriptional regulation of ANKRD22 modulates mitochondrial function and induction of CRC cell stemness, providing new insights into CRC pathogenesis and potential therapeutic targets. However, it remains to be determined whether this regulatory mechanism operates through the modulation of mitochondrial homeostasis, which in turn may influence stem cell stemness and contribute to CRC progression. Thus, further mechanistic verification in this regard is required.

Availability of Data and Materials

The analyzed data sets generated during the study are available from the corresponding author on reasonable request.

Author Contributions

XZ, YX and YZ designed the research study; QX and YX performed the research; SL and PS collected and analyzed the data. YX has been involved in drafting the manuscript and all authors have been involved in revising it critically for important intellectual content. All authors give final approval of the version to be published. All authors have participated sufficiently in the work to take public responsibility for appropriate portions of the content and agreed to be accountable for all aspects of the work in ensuring that questions related to its accuracy or integrity are addressed.

Ethics Approval and Consent to Participate

Not applicable.

Acknowledgment

Not applicable.

Funding

This research received no external funding.

Conflict of Interest

The authors declare no conflict of interest.

Supplementary Material

Supplementary material associated with this article can be found, in the online version, at https://doi.org/10.24976/Discov.Med.202537202.232.

References

[1] Corrales L, Hipp S, Martin K, Sabarth N, Tirapu I, Fuchs K, *et al*. LY6G6D is a selectively expressed colorectal cancer antigen that can be used for targeting a therapeutic T-cell response by a T-cell engager. Frontiers in Immunology. 2022; 13: 1008764. https://doi.org/10.3389/fimmu.2022.1008764.

[2] Zhang Y, Guan H, Feng X, Liu M, Shao J, Liu M, *et al*. Emerging strategies in colorectal cancer immunotherapy: enhancing efficacy and survival. Frontiers in Immunology. 2025; 16: 1616414. https://doi.org/10.3389/fimmu.2025.1616414.

[3] Vekic B, Dragojevic-Simic V, Jakovljevic M, Kalezic M, Zagorac Z, Dragovic S, *et al*. A Correlation Study of the Colorectal Cancer Statistics and Economic Indicators in Selected Balkan Countries. Frontiers in Public Health. 2020; 8: 29. https://doi.org/10.3389/fpubh.2020.00029.

[4] Feng RM, Zong YN, Cao SM, Xu RH. Current cancer situation in China: good or bad news from the 2018 Global Cancer Statistics? Cancer Communications (London, England). 2019; 39: 22. https://doi.org/10.1186/s40880-019-0368-6.

[5] Madan B, Ke Z, Harmston N, Ho SY, Frois AO, Alam J, *et al*. Wnt addiction of genetically defined cancers reversed by PORCN inhibition. Oncogene. 2016; 35: 2197–2207. https://doi.org/10.1038/onc.2015.280.

[6] Shen X, Zhang Y, Xu Z, Gao H, Feng W, Li W, *et al*. KLF5 inhibition overcomes oxaliplatin resistance in patient-derived colorectal cancer organoids by restoring apoptotic response. Cell Death & Disease. 2022; 13: 303. https://doi.org/10.1038/s41419-022-04773-1.

[7] Zhou W, Huang Y, Liu J, Liu Y, Liu Y, Yu C. Identification of ANKRD13D as a potential target in renal cell carcinomas. The International Journal of Biological Markers. 2024; 39: 149–157. https://doi.org/10.1177/03936155241236498.

[8] Wang R, Wu Y, Zhu Y, Yao S, Zhu Y. ANKRD22 is a novel therapeutic target for gastric mucosal injury. Biomedicine & Pharmacotherapy = Biomedecine & Pharmacotherapie. 2022; 147: 112649. https://doi.org/10.1016/j.biopha.2022.112649.

[9] Takahashi A, Seike M, Chiba M, Takahashi S, Nakamichi S, Matsumoto M, *et al*. Ankyrin Repeat Domain 1 Overexpression is Associated with Common Resistance to Afatinib and Osimer-

tinib in EGFR-mutant Lung Cancer. Scientific Reports. 2018; 8: 14896. https://doi.org/10.1038/s41598-018-33190-8.

[10] Traina F, Favaro PMB, Medina SDS, Duarte ADSS, Winnischofer SMB, Costa FF, *et al*. ANKHD1, ankyrin repeat and KH domain containing 1, is overexpressed in acute leukemias and is associated with SHP2 in K562 cells. Biochimica et Biophysica Acta. 2006; 1762: 828–834. https://doi.org/10.1016/j.bbadis.2006.07.010.

[11] Lim SP, Wong NC, Suetani RJ, Ho K, Ng JL, Neilsen PM, *et al*. Specific-site methylation of tumour suppressor ANKRD11 in breast cancer. European Journal of Cancer (Oxford, England: 1990). 2012; 48: 3300–3309. https://doi.org/10.1016/j.ejca.2012.03.023.

[12] Wu Y, Ruggiero CL, Bauman WA, Cardozo C. Ankrd1 is a transcriptional repressor for the androgen receptor that is downregulated by testosterone. Biochemical and Biophysical Research Communications. 2013; 437: 355–360. https://doi.org/10.1016/j.bbrc.2013.06.079.

[13] Bai R, Li D, Shi Z, Fang X, Ge W, Zheng S. Clinical significance of Ankyrin repeat domain 12 expression in colorectal cancer. Journal of Experimental & Clinical Cancer Research: CR. 2013; 32: 35. https://doi.org/10.1186/1756-9966-32-35.

[14] Ma J, Chen S, Su M, Wang W. High FN1 expression is associated with poor survival in esophageal squamous cell carcinoma. Medicine. 2023; 102: e33388. https://doi.org/10.1097/MD.0000000000033388.

[15] Pan T, Liu J, Xu S, Yu Q, Wang H, Sun H, *et al*. ANKRD22, a novel tumor microenvironment-induced mitochondrial protein promotes metabolic reprogramming of colorectal cancer cells. Theranostics. 2020; 10: 516–536. https://doi.org/10.7150/thno.37472.

[16] Wanet A, Arnould T, Najimi M, Renard P. Connecting Mitochondria, Metabolism, and Stem Cell Fate. Stem Cells and Development. 2015; 24: 1957–1971. https://doi.org/10.1089/scd.2015.0117.

[17] Wang Z, Song Y, Zhang H, Yang Y, Zhang S, Wang W. Local anesthetic levobupivacaine inhibits stemness of osteosarcoma cells by epigenetically repressing MAFB though reducing KAT5 expression. Aging. 2022; 14: 2793–2804. https://doi.org/10.18632/aging.203975.

[18] Porporato PE, Payen VL, Pérez-Escuredo J, De Saedeleer CJ, Danhier P, Copetti T, *et al*. A mitochondrial switch promotes tumor metastasis. Cell Reports. 2014; 8: 754–766. https://doi.org/10.1016/j.celrep.2014.06.043.

[19] Mira RG, Quintanilla RA, Cerpa W. Mild Traumatic Brain Injury Induces Mitochondrial Calcium Overload and Triggers the Upregulation of NCLX in the Hippocampus. Antioxidants (Basel, Switzerland). 2023; 12: 403. https://doi.org/10.3390/antiox12020403.

[20] Yukimoto R, Nishida N, Hata T, Fujino S, Ogino T, Miyoshi N, *et al*. Specific activation of glycolytic enzyme enolase 2 in BRAF V600E-mutated colorectal cancer. Cancer Science. 2021; 112: 2884–2894. https://doi.org/10.1111/cas.14929.

[21] Pecce V, Verrienti A, Fiscon G, Sponziello M, Conte F, Abballe L, *et al*. The role of FOSL1 in stem-like cell reprogramming processes. Scientific Reports. 2021; 11: 14677. https://doi.org/10.1038/s41598-021-94072-0.

[22] Livak KJ, Schmittgen TD. Analysis of relative gene expression data using real-time quantitative PCR and the 2(-Delta Delta C(T)) Method. Methods (San Diego, Calif.). 2001; 25: 402–408. https://doi.org/10.1006/meth.2001.1262.

[23] Liu X, Zhao J, Wu Q, Wang L, Lu W, Feng Y. ANKRD22 promotes glioma proliferation, migration, invasion, and epithelial-mesenchymal transition by upregulating E2F1-mediated MELK expression. Journal of Neuropathology and Experimental Neurology. 2023; 82: 631–640. https://doi.org/10.1093/jnen/nlad034.

[24] Huynh HTLK, Lim HGM, Lee YCG, Phan TV, Vo TH, Chen CH, *et al*. *In Silico* Identification of ANKRD22 as a Theragnostic Target for Pancreatic Cancer and Fostamatinib's Therapeutic Potential. International Journal of Medical Sciences. 2025; 22: 1885–1904. https://doi.org/10.7150/ijms.105193.

[25] Yin J, Fu W, Dai L, Jiang Z, Liao H, Chen W, *et al*. ANKRD22 promotes progression of non-small cell lung cancer through transcriptional up-regulation of E2F1. Scientific Reports. 2017; 7: 4430. https://doi.org/10.1038/s41598-017-04818-y.

[26] Chen J, Wu Z, Deng W, Tang M, Wu L, Lin N, *et al*. USP51 promotes non-small cell lung carcinoma cell stemness by deubiquitinating TWIST1. Journal of Translational Medicine. 2023; 21: 453. https://doi.org/10.1186/s12967-023-04304-2.

[27] Wang D, Fu L, Wei J, Xiong Y, DuBois RN. PPARδ Mediates the Effect of Dietary Fat in Promoting Colorectal Cancer Metastasis. Cancer Research. 2019; 79: 4480–4490. https://doi.org/10.1158/0008-5472.CAN-19-0384.

[28] Fujino S, Miyoshi N. Oct4 Gene Expression in Primary Colorectal Cancer Promotes Liver Metastasis. Stem Cells International. 2019; 2019: 7896524. https://doi.org/10.1155/2019/7896524.

[29] Li H, Dai W, Xia X, Wang R, Zhao J, Han L, *et al*. Modeling tumor development and metastasis using paired organoids derived from patients with colorectal cancer liver metastases. Journal of Hematology & Oncology. 2020; 13: 119. https://doi.org/10.1186/s13045-020-00957-4.

[30] De Francesco EM, Sotgia F, Lisanti MP. Cancer stem cells (CSCs): metabolic strategies for their identification and eradication. The Biochemical Journal. 2018; 475: 1611–1634. https://doi.org/10.1042/BCJ20170164.

[31] Sahoo BM, Banik BK, Borah P, Jain A. Reactive Oxygen Species (ROS): Key Components in Cancer Therapies. Anticancer Agents in Medicinal Chemistry. 2022; 22: 215–222. https://doi.org/10.2174/1871520621666210608095512.

[32] Moon DO. Calcium's Role in Orchestrating Cancer Apoptosis: Mitochondrial-Centric Perspective. International Journal of Molecular Sciences. 2023; 24: 8982. https://doi.org/10.3390/ijms24108982.

[33] Nayakanti SR, Friedrich A, Sarode P, Jafari L, Maroli G, Boehm M, *et al*. Targeting Wnt-ß-Catenin-FOSL Signaling Ameliorates Right Ventricular Remodeling. Circulation Research. 2023; 132: 1468–1485. https://doi.org/10.1161/CIRCRESAHA.122.321725.

[34] Zhao H, Ming T, Tang S, Ren S, Yang H, Liu M, *et al*. Wnt signaling in colorectal cancer: pathogenic role and therapeutic target. Molecular Cancer. 2022; 21: 144. https://doi.org/10.1186/s12943-022-01616-7.

[35] Dai FQ, Li CR, Fan XQ, Tan L, Wang RT, Jin H. miR-150-5p Inhibits Non-Small-Cell Lung Cancer Metastasis and Recurrence by Targeting HMGA2 and β-Catenin Signaling. Molecular Therapy. Nucleic Acids. 2019; 16: 675–685. https://doi.org/10.1016/j.omtn.2019.04.017.

[36] Vallée A, Vallée JN, Guillevin R, Lecarpentier Y. Riluzole: a therapeutic strategy in Alzheimer's disease by targeting the WNT/β-catenin pathway. Aging. 2020; 12: 3095–3113. https://doi.org/10.18632/aging.102830.